ENERGY RECOVERY STRATEGIES FOR CONTINUOUS MIXED-FLOW GRAIN DRYERS OPTIMIZATION

George STANESCU, stanescu@ufpr.br
Federal University of Paraná, Mechanical Engineering Department, 81531-990 Curitiba, PR, Brazil

Marcelo Risso ERRERA, errera@ufpr.br
Federal University of Paraná, Environmental Engineering Department, 81531-990 Curitiba, PR, Brazil

Abstract. *In 2011 the Brazilian industry will pre-process more than 50% of its 150 millions tones of grains harvest. In terms of potential of energy resources consumption, this represents more than 10^4 TJ of thermal energy/year. That alone dramatically increased the need for more efficient drying technologies. This paper is a sequence of continuing efforts to optimize grain drying plants that now presents the investigation of two different strategies for energy recovery in continuous mixed-flow grain dryers. Use of 1st and 2nd Laws of Thermodynamics on control volumes lead to an algebraic non-linear model that was solved iteratively. Numerical results obtained for the soybean drying process yield energy efficiencies of 2.8-3.5 MJ/ (kg of vaporized water), while the heater consumption varies from 4.7 to 5.7 Nm^3 CH_4/ (ton of dried soybean).*

Keywords*: energy efficiency, energy recovery strategies, grain drying optimization, continuous mixed-flow grain dryers*

1. INTRODUCTION

In this paper we considered the use of energy in grain drying plants, one of the most intensive energy consumption industrial processes.

To optimize grain drying plants we firstly addressed the problem of determining the best strategy to deliver drying gas to the drying chamber in order to maximize the utilization of the drying gas moisture removal and carrying capability (Stanescu and Errera, 2010). We determined the best strategy to delivery the minimum drying gas flow rate that balanced internal moisture diffusion with external convection mass transfer.

The objective function already maximized in that earlier step is the drying air specific humidity in kilograms of vaporized moisture per kilograms of drying gas. Results shed light on sizing drying chambers such that the using of drying gas moisture carrying capability almost doubles while the drying gas mass flow rate decreases six times.

Numerical values of calculated thermal efficiency indicate a potential improvement to 14.28% (with constant drying air delivery) and further to 27.53% when the best variable drying air delivery strategy is employed.

The present work shows two new ways of enhancing energy performance of continuous-mixed dryers as whole equipment. The study departs from already optimized drying chambers from our earlier work assembled with four auxiliary devices.

The drying plant (or dryer) is formed by a sequence of four unitary processes that take place inside an air heater, a drying chamber, a heat exchanger and a cooling chamber (Fig. 1).

The first strategy to increase the energy efficiency of the whole drying plant considered in this paper takes into account that some of the internal energy of the wet drying air that leaves the drying chamber is recovered in a heat exchanger by ambient air flow that afterwards flows to a main air heater (Fig. 1a).

The second strategy considers the operational requirement to cool down dried grains before moving them to storage. That is necessary since warm dried grains absorb moisture from ambient air while cooling down. We thus considered that some of the internal energy of the warm dried grains is recovered by ambient air flow that afterwards flows to the heat exchanger introduced by the first strategy (Fig. 1b).

Numerical results of the algebraic system are compared for the same continuous mixed-flow grain dryer when the two strategies for energy recovery allow warm air and cooled drying air, or warm air, cooled drying air and condensed liquid water to leave the heat exchanger.

2. ANALYSIS OF A GRAIN DRYING PLANT

As shown in Fig. 1, the sequence of unitary processes in a continuous mixed-flow dryer is given by the processes occurring inside four control volumes: the heater, the optimized drying chamber, the heat exchanger and the cooling chamber.

The dryer model considered for this paper makes use of gravity to move grains throughout the drying chamber. The drying chamber, where the moisture from grains is effectively removed, is crossed along vertical direction by wet grains flow and horizontally by the hot drying gas flow. Process throughout the drying chamber reduces the grains moisture content while simultaneously increases the grains temperature.

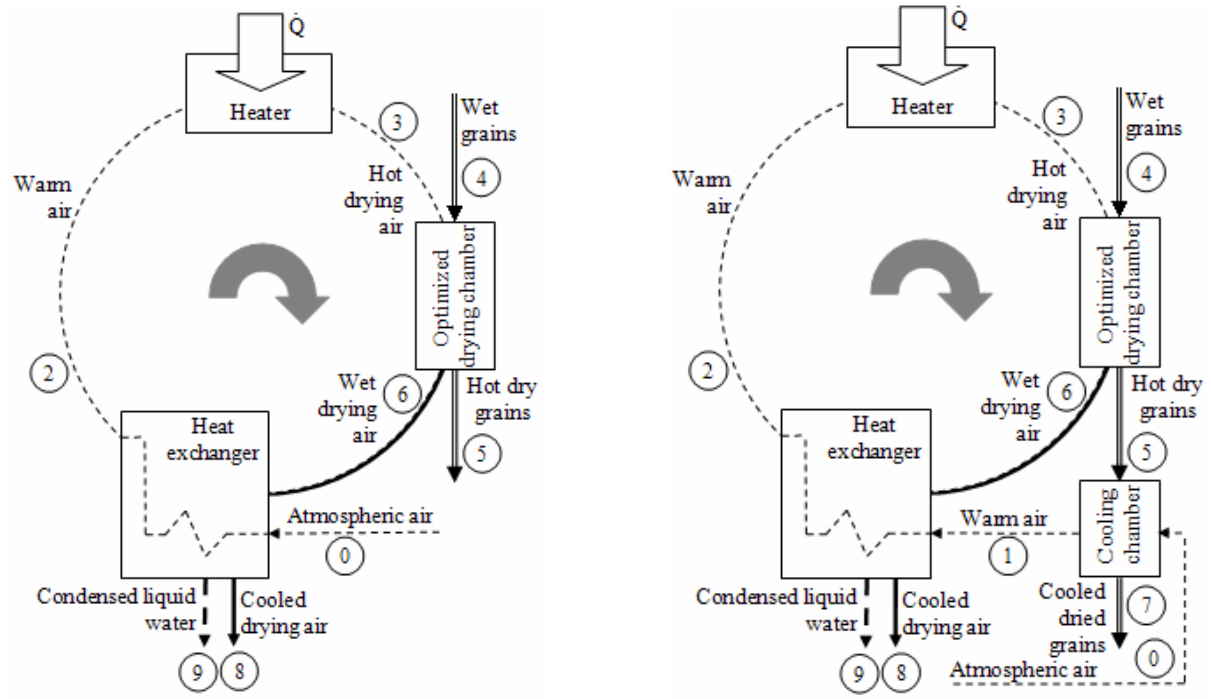

Figure 1. The humid drying air internal energy recovery strategy (a) and the humid drying air and hot dry grains internal energy recovery strategy (b).

During the process of moisture removal some of the internal energy of the hot, low relative humidity, drying gas is used to evaporate the grains liquid water content. Still part of the enthalpy of the hot air plays no role in the drying process.

Some of its internal energy is recovered in the heat exchanger by the ambient air inflow as outlined in Fig. 1a to increase the energy efficiency of the whole drying plant.

The process inside the heat exchanger allows to gradually increases the atmospheric airflow temperature before it enters the heater (streams are not mixed).

In order to avoid that already dried grains naturally absorb moisture from the atmosphere during the storage, they are cooled down to ambient temperature in the cooling chamber before leaving the dryer. Similarly to the heat exchanger process, to improve the drying plant energy efficiency, the second strategy assumes that some of the grains internal energy, removed during the grains cooling down, is transferred to the preheated atmospheric airflow before it enters the heaters (Fig. 1b).

2.1. Physical Model

To maximize the utilization of the drying gas moisture removal and carrying capability, and to optimize the drying chamber, our first study focused on the grains moisture removal process inside the drying chamber (Stanescu and Errera, 2010).

The internal architecture of the drying chamber has been decomposed into a repetitive structure of many adjacent simple column drying chambers each one representing a three-dimensional domain crossed vertically by the moving layer of grains and horizontally by the drying gas flow.

We then optimized the simple column drying chamber and evaluate the effectiveness of the variable drying air delivery strategy to reduce the grain drying specific energy consumption. The drying chamber was divided into n × k elemental control volumes (W × L/k × H/n) as shown in Fig. 2.

All together the k elemental control volumes labeled (i, 1≤j≤k) along the horizontal direction form a W × L × H/n "slice". The optimal dimensionless drying air mass flow rate ($\tilde{m}_a$), hot drying gas specific humidity (ω), hot drying gas relative humidity (ϕ), hot drying gas temperature (T), and grains relative humidity (M) internal distribution along each "slice" have been numerically determined.

Each "slice" along the horizontal direction is considered to be a unitary optimized drying chamber equipped with unitary heat exchanger and heater as shown in Figures 3a and 3b. In this study we determine the minimal consumption of methane to ensure the whole drying plant functioning based on the already known parameters.

2.2. Mathematical Model

We firstly studied the simple column drying chamber shown in Fig. 2 with fixed overall dimensions of width and length (W × L) and variable height H, constant mass flow rate of moist grains at the entrance and constant hot drying gas temperature. The drying process reduces the grains moisture content (kg water/kg dry solid) from a specific initial value M_0 (at the top) to a final fixed value M_f (at the bottom). The grain bed with a bulk density ρ_g slowly moves downward by gravity. The grains bed linear velocity U_g is aligned with H while the hot drying air cross-flow is aligned with L.

The mathematical problem consisted of computing the temperature of the grains, the temperature of the drying gas, the grains moisture content and the drying gas relative humidity distributions throughout the L × H domain.

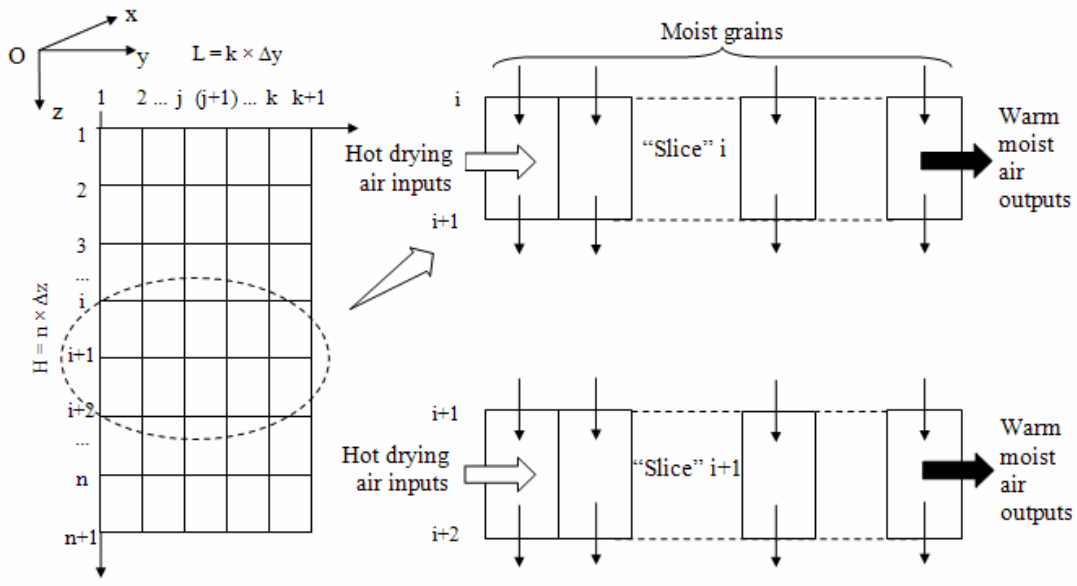

Figure 2. Discretization of the physical domain.

The model considered the following hypotheses:

- steady-state functioning of the grains dryer;
- drying air flows mainly along the *Oy* direction;
- grains flow mainly along the *Oz* direction;
- internal diffusion is the predominant mechanism of mass transfer inside the grains;
- mass transfer between the grains external surface and the drying gas is limited by the moisture carrying capability of the drying air and it is constrained by the grains equilibrium moisture content;
- thermodynamic equilibrium between the solid and liquid phases;
- instantaneous thermodynamic equilibrium between the drying gas and the vaporized moisture;
- all streams throughout the dryer are assumed constant pressure flows;
- empirical grains temperature linear distribution along the *Oz* direction already available in the literature is used to simplify the modeling;
- heat losses are negligible;
- grains flow mass rate is uniform.

The mathematical model employed derived from the equations of mass and energy conservation applied throughout the simple column drying chamber. Numerical integration of the mathematical model was performed based on a coupled control volumes method to discretize the simple column drying chamber domain.

The drying air mass flow rates are determined when constant and variable drying gas mass flow rate delivery strategies are considered. The hot drying gas absolute humidity, the hot drying gas relative humidity, the hot drying gas temperature, and the grains relative humidity internal distribution throughout the simple column dryer are also numerically determined. The mathematical model used in this study is also represented by the mass and energy balance equations written down for the steady state functioning of the cooling chamber and each one of the n heat exchangers and the n heaters in Figure 3.

Table 1 presents the algebraic formulation of the mass and energy balance equations used to study the continuous mixed-flow grain dryer with optimized drying chamber when the wet drying air internal energy recovery strategy is

employed. Mass and energy balance equations shown in Table 2 are considered when the wet drying air and hot dry grains internal energy recovery strategy is employed to increase the energy efficiency of the continuous mixed-flow grain dryer with optimized drying chamber. Both mathematical models are employed in this study focusing on determining the best energy recovery strategy to reduce the continuous mixed-flow grain dryer methane expenditure.

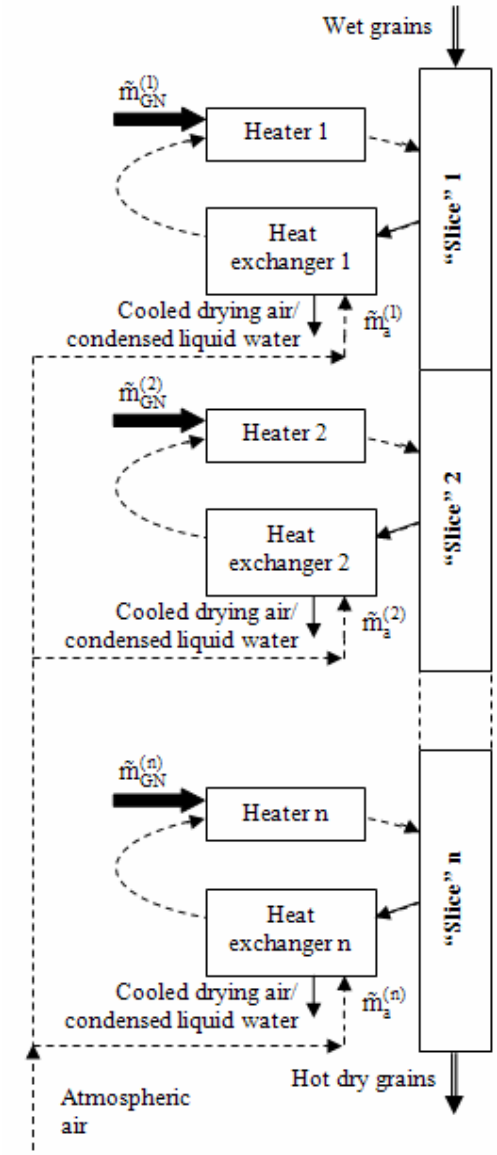

Figure 3a. Wet drying air internal energy recovery strategy for a continuous mixed-flow grain dryer with optimized drying chamber.

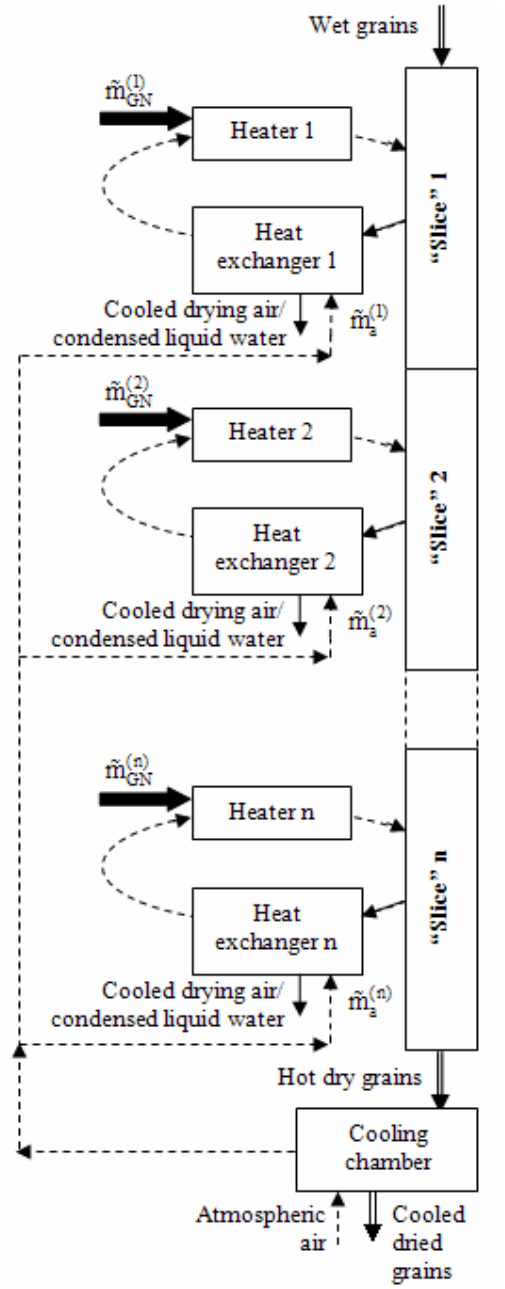

Figure 3b. Wet drying air and hot dry grains internal energy recovery strategy for a continuous mixed-flow grain dryer with optimized drying chamber.

3. NUMERICAL PROCEDURE

Numerical values in Table 3, used to determine solutions of both mathematical models, are provided based on a previous study focused on maximizing utilization of the drying gas moisture removal and carrying capability (Stanescu and Errera, 2010). Employing relations already available in the literature to evaluate the equilibrium moisture content (Lira et al., 2009) and the effective mass diffusivity of water inside the grains (Barrozo et al., 2006) the numerical

integration was performed until $\left|(\tilde{T}_6^{i+1}-\tilde{T}_6^{i})/\tilde{T}_6^{i+1}\right|\le 10^{-3}$ and $\left|(\omega_6^{i+1}-\omega_6^{i})/\omega_6^{i+1}\right|\le 10^{-3}$. The mathematical model consisting of Eqs. (1), (2), (5) and (6), solved for residuals less than 10^{-3}, is employed to study firstly the wet drying air internal energy recovery strategy when only cooled drying air leaves each one of the n heat exchangers. Based on the previously determined (Table 3) hot drying gas absolute humidity $\omega_6^{(i,k+1)}$ in Eq. (1), we calculated the cooled drying air temperature $T_8^{(i)*}$ when leaving the "i" heat exchanger. Then, based on the numerical values of $\omega_6^{(i,k+1)}$, $T_6^{(i,k+1)}$ and $T_8^{(i)*}$ we determine from Eq. (2) the temperature of the warm air leaving the "i" heat exchanger $T_2^{(i)*}$. Dimensionless dry air mass flow rate $\tilde{m}_a^{(i)}$ allows determinations of the $n_j^{(i)}$ coefficients in Eq. (5) and then calculation from Eq. (6) of dimensionless natural gas consumption $\tilde{m}_{NG}^{(i)}$ by the "i" heater. Consumption of methane for the whole drying plant is calculated by adding the $\tilde{m}_{NG}^{(i)}$ terms for all heaters. In Eq. (2) c_{pa} and h_w represent respectively the mass specific heat at constant pressure of the dry air and the mass specific enthalpy of the slightly superheated water vapor, while $\bar{h}$ represents in Eq. (6) the molal specific enthalpy. Approximation by the saturated-vapor properties at the same temperature of properties of water slightly superheated-vapor is used is this study to calculate specific enthalpies of water vapor (Bejan, 1997).

Table 1. Mass and energy balance equations to study the wet drying air internal energy recovery strategy.

	Mass balance equation	Energy balance equation	Observations
The "i" heat exchanger when only cooled drying air leaves the equipment	$\omega_6^{(i,k+1)}=0.622P_{sat}(T_8^{(i)*})/[P_0-P_{sat}(T_8^{(i)*})]$ Eq. (1)	$c_{pa}(T_0+T_6^{(i,k+1)}-T_2^{(i)*}-T_8^{(i)*})+\omega_0[h_w(T_0)-h_w(T_2^{(i)*})]+\omega_6^{(i,k+1)}[h_w(T_6^{(i,k+1)})-h_w(T_8^{(i)*})]=0$ Eq. (2)	$\phi_8^{(i)}=1$ $\omega_8^{(i)}=\omega_6^{(i,k+1)}$ $\omega_2^{(i)}=\omega_0$
The "i" heat exchanger when cooled drying air and condensed liquid water leave the equipment	$\omega_8^{(i)}=0.622P_{sat}(T_8^{(i)**})/[P_0-P_{sat}(T_8^{(i)**})]$ Eq. (3)	$c_{pa}(T_0+T_6^{(i,k+1)}-T_2^{(i)**}-T_8^{(i)**})+\omega_0[h_w(T_0)-h_w(T_2^{(i)**})]+\omega_6^{(i,k+1)}h_w(T_6^{(i,k+1)})-\omega_8^{(i)}h_w(T_8^{(i)**})-(\omega_6^{(i,k+1)}-\omega_8^{(i)})h_{w,liq}(T_9^{(i)})=0$ Eq. (4)	$\phi_8^{(i)}=1$ $\omega_8^{(i)}<\omega_6^{(i,k+1)}$ $\omega_2^{(i)}=\omega_0$ $T_0<T_8^{(i)**}$ $T_8^{(i)**}<T_8^{(i)*}$ $T_6^{(i,k+1)}>T_2^{(i)**}$ $T_2^{(i)**}>T_2^{(i)*}$ $T_9^{(i)}=T_8^{(i)**}$
The "i" heater	$1.81\tilde{m}_{NG}^{(i)}CH_4+\tilde{m}_a^{(i)}(0.21O_2+0.79N_2+1.61\omega_0H_2O)\rightarrow 1.81\tilde{m}_{NG}^{(i)}CO_2+(3.62\tilde{m}_{NG}^{(i)}+1.61\omega_0\tilde{m}_a^{(i)})H_2O+(0.21\tilde{m}_a^{(i)}-3.62\tilde{m}_{NG}^{(i)})O_2+0.79\tilde{m}_a^{(i)}N_2$ Eq. (5)	$\sum_{j=CH_4,O_2,N_2}^{H_2O}\tilde{n}_j^{(i)}\bar{h}_{j,2}=\sum_{j=CO_2,H_2O,O_2}^{N_2}\tilde{n}_j^{(i)}\bar{h}_j(T_3)$ Eq. (6)	The heater functions as a combustion chamber

When the same strategy of the wet drying air internal energy recovery is employed, but allowing drying air and some condensed liquid water to leave each one of the n heat exchangers, we use the mathematical model represented by Eqs. (3), (4), (5) and (6) to determine the drying plant NG consumption. Based on guessed values of $T_8^{(i)**}$, $T_0<T_8^{(i)**}<T_8^{(i)*}$ we iteratively calculate $\omega_8^{(i)}$ from Eq. (3) until the temperature of the warm air leaving the "i" heat exchanger in Eq. (4) reaches the highest possible value $T_2^{(i)**}$ with $T_6^{(i,k+1)}>T_2^{(i)**}>T_2^{(i)*}$. Now, based on the already known values of $\omega_6^{(i,k+1)}$ and $T_6^{(i,k+1)}$, and on the lower possible values of $T_8^{(i)*}$ and the highest possible value

$T_2^{(i)**}$ we balance the $n_j^{(i)}$ coefficients in Eq. (5) and then calculate from Eq. (6) the dimensionless natural gas consumption $\tilde{m}_{NG}^{(i)}$ into the "i" heater. Consumption of the NG for the whole drying plant is again calculated by adding the $\tilde{m}_{NG}^{(i)}$ terms.

Numerical procedure employed to study the wet drying air and hot dry grains internal energy recovery strategy mathematically differs from the already discussed procedures only by the drying air temperature when entering the heat exchangers. Until now, we accounted for the atmospheric air at T_0=20^{0}C, pressure $P_0 = 10^5$ Pa and relative humidity φ_0 = 60 % to enters each one o the n heat exchangers. The wet drying air and hot dry grains internal energy recovery strategy assumes that each one of the n heat exchangers receive warm air already heated up to T_1 into the cooling chamber. Temperature T_1 of the warm air is determined from Eq. (7) based on the already known values of $\tilde{m}_a^{(i)}$, $T_5^{(n+1)}$ and $M_5^{(n+1)}$. Numerical value of T_1 calculated based on Eq. (7) is now used to solve the mathematical model represented by Eqs. (8), (9), (5) and (6) when only cooled drying air leaves the n heat exchangers, or the mathematical model of Eqs. (10), (11), (5) and (6) when drying air and some condensed liquid water leave the heat exchangers.

Table 2. Mass and energy balance equations to study wet drying air and hot dry grains internal energy recovery strategy.

	Mass balance equation	Energy balance equation	Observations
The cooling chamber	The mass conservation is guaranteed before hand by assuming no mass transfer between grains and the atmospheric air	$\left(\sum_{i=1}^{n}\tilde{m}_a^{(i)}\right)\times[c_{pa}(T_0-T_1)+\omega_0(h_w(T_0)-h_w(T_1))]+c_{pg}(T_5^{(n+1)}-T_7)+M_5^{(n+1)}\times[h_{w,liq}(T_5^{(n+1)})-h_{w,liq}(T_7)]=0$ Eq. (7)	$\omega_1=\omega_0$ $M_7=M_5^{(n+1)}$ $T_7=T_0$
The "i" heat exchanger when only cooled drying air leaves the equipment	$\omega_6^{(i,k+1)}=0.622P_{sat}(T_8^{(i)*})/[P_0-P_{sat}(T_8^{(i)*})]$ Eq. (8)	$c_{pa}(T_1+T_6^{(i,k+1)}-T_2^{(i)*}-T_8^{(i)*})+\omega_1[h_w(T_1)-h_w(T_2^{(i)*})]+\omega_6^{(i,k+1)}[h_w(T_6^{(i,k+1)})-h_w(T_8^{(i)*})]=0$ Eq. (9)	$\phi_8^{(i)}=1$ $\omega_8^{(i)}=\omega_6^{(i,k+1)}$ $\omega_2^{(i)}=\omega_1$
The "i" heat exchanger when cooled drying air and condensed liquid water leave the equipment	$\omega_8^{(i)}=0.622P_{sat}(T_8^{(i)**})/[P_0-P_{sat}(T_8^{(i)**})]$ Eq. (10)	$c_{pa}(T_1+T_6^{(i,k+1)}-T_2^{(i)**}-T_8^{(i)**})+\omega_1[h_w(T_1)-h_w(T_2^{(i)**})]+\omega_6^{(i,k+1)}h_w(T_6^{(i,k+1)})-\omega_8^{(i)}h_w(T_8^{(i)**})-(\omega_6^{(i,k+1)}-\omega_8^{(i)})h_{w,liq}(T_9^{(i)})=0$ Eq. (11)	$\phi_8^{(i)}=1$ $\omega_8^{(i)}<\omega_6^{(i,k+1)}$ $\omega_2^{(i)}=\omega_1$ $T_1<T_8^{(i)**}$ $T_8^{(i)**}<T_8^{(i)*}$ $T_6^{(i,k+1)}>T_2^{(i)**}$ $T_2^{(i)**}>T_2^{(i)*}$ $T_9^{(i)}=T_8^{(i)**}$
The "i" heater	Eq. (5)	Eq. (6)	The heater functions as a combustion chamber

4. RESULTS AND DISCUSSION

Numerical results in this paper are calculated for industrial soybeans dryers operation. In order to optimize

energetically the functioning of such plants, results based on the mathematical model presented in this paper are further employed to maximize the productivity of actual soybeans drying systems.

Typical values for industrial soybeans dryers functioning considered in here are the initial grains moisture content M_0 = 22% (dry basis) and the final moisture content M_f = 15%, the atmospheric conditions $T_0 = 20\ ^0C$, $P_0 = 10^5$ Pa, ϕ_0 = 60 %, $\omega_0 = 0.0089$ and the drying gas temperature $T_3 = 90\ ^0C$ at the drying chamber entrance.

Table 3. Numerical results already calculated for the continuous mixed-flow grain dryer with variable drying gas mass flow rate delivering strategy to the optimized drying chamber ($n = 570$, $k = 40$, $\tilde{T}_5^{(n+1)} = 1.684$, $M_5^{(n+1)} = 0.14941$)

i	$\tilde{m}_a^{(i)}$	$\omega_6^{(i,k+1)}$	$\tilde{T}_6^{(i,k+1)}$
1	7.5752	0.03119	1.78
2	3.7807	0.03107	1.79
3	2.6620	0.03098	1.78
4	2.1710	0.03091	1.78
5	1.8655	0.03085	1.78
8	1.3983	0.03071	1.78
9	1.3045	0.03067	1.78
10	1.2255	0.03063	1.78
11	1.1594	0.03060	1.78
12	1.1026	0.03056	1.78
39	0.5536	0.02991	1.78
77	0.3655	0.02928	1.77
115	0.2828	0.02876	1.76
267	0.1591	0.02709	1.73
343	0.1325	0.02636	1.72
419	0.1139	0.02567	1.70
533	0.0942	0.02467	1.67
570	0.0913	0.02433	1.66

Firstly we evaluated the effectiveness of the variable drying air delivering strategy to reduce the grain drying specific energy consumption and compared the thermal efficiency of the simple column drying chamber for both, the constant and the variable drying gas mass flow rate cases.

Hot drying gas absolute humidity, the hot drying gas relative humidity, the hot drying gas temperature, and the grains relative humidity numerical values already determined during this first approach are now used to investigate the best energy recovery strategy in order to minimize the NG consumption of the whole drying plant when both, the wet drying air internal energy recovery strategy and the wet drying air and hot dry grains internal strategy are considered for a continuous mixed-flow grain dryer with optimized drying chamber.

Table 4 show the numerical results calculated for both, the wet drying air internal energy recovery strategy and the wet drying air and hot dry grains internal strategy applied to a continuous mixed-flow grain dryer with optimized drying chamber.

Based on the minimum NG consumption of the whole drying plant (4.7108 Nm^3 CH_4/ton of dried soybean) it is worth noting in Table 4 to candidates to the best strategy label, the wet drying air internal energy recovery strategy and the wet drying air and hot dry grains internal energy recovery strategy when drying air and condensed liquid water leave the heat exchangers.

The worst situation corresponds to the continuous mixed-flow grain dryer functioning based on the wet drying air internal energy recovery strategy, allowing only cooled drying air to leave the heat exchangers, when the NG consumption of the whole drying plant increases almost 21% at 5.7046 Nm^3 CH_4/ton of dried soybean.

The amount of condensed liquid water generated when using the wet drying air and hot dry grains internal energy recovery strategy is approximately three times lower when compared with those generated when the wet drying air internal energy recovery strategy is employed.

Table 4. Numerical results calculated for both, the wet drying air internal energy recovery strategy and the wet drying air and hot dry grains internal strategy applied to a continuous mixed-flow grain dryer with optimized drying chamber

Strategy	$\frac{\dot{Q}}{(M_0 - M_f)\dot{m}_g}$	$\frac{22.414\sum_{i=1}^{n}\tilde{m}_{GN}^{(i)}}{16\times(1+M_f)}$	$\frac{\sum_{i=1}^{n}(\omega_6^{(i,k+1)} - \omega_8^{(i)})\tilde{m}_a^{(i)}}{(1+M_f)}$
	$\left(\frac{\text{kJ}}{\text{kg vaporized water}}\right)$	$\left(\frac{\text{Nm}^3\ CH_4}{\text{ton of dried soybean}}\right)$	$\left(\frac{\text{kg condensed liquid water}}{\text{ton of dried soybean}}\right)$
Wet drying air internal energy recovery strategy	3,459.98	5.7046	Only cooled drying air leaves the heat exchangers
	2,858.34	4.7108	11.1037
Wet drying air and hot dry grains internal energy recovery strategy	3,084.00	5.0835	Only cooled drying air leaves the heat exchangers
	2,858.34	4.7108	3.8108

5. CONCLUSIONS

This study represents the second step of optimization actions for a continuous mixed-flow grain dryer with already optimized drying chamber. The first step optimization focused on maximizing the utilization of the drying gas moisture removal and its carrying capability. Then we studied the best drying gas mass flow rate delivering strategy to determine the minimum drying gas mass flow rate to the drying chamber to maintain balanced the internal mass diffusion and external convection mass transfer. Numerical values of calculated thermal efficiency indicated a potential improvement from 14.28% for constant drying air delivering up to 27.53% when the best variable drying air delivering strategy is employed. The first step optimization shed light on sizing drying chambers such that the drying gas moisture carrying capability almost double while the drying gas mass flow rate decreases six times. This paper presents the second step of the continuous mixed-flow grain dryer optimization process assuming the drying chamber already optimized based on variable drying gas mass flow rate delivering. The objective function to be minimized is now the methane consumption of the whole drying plant when both, the wet drying air internal energy recovery strategy and the wet drying air and hot dry grains internal strategy are considered.

In order to increase the energy efficiency of the whole drying plant the first strategy considers that some of the internal energy of the wet drying air that leaves the drying chamber is recovered in the heat exchanger by the ambient air flow before it enters the heater. The second strategy, to avoid that already dried grains naturally gain moisture from the ambient air during the storage, assumes that some of the grains internal energy is removed when leaving the dryer by the ambient air flow before it enters the heat exchanger. Numerical results are calculated for the same continuous mixed-flow grain dryer when the two strategies for energy recovery allow warm air and cooled drying air, or warm air, cooled drying air and condensed liquid water to leave the heat exchanger. The minimum methane consumption of the whole drying plant is calculated at 4.7108 Nm^3 CH_4/ton of dried soybean and there are two candidates to the best strategy, namely, the wet drying air internal energy recovery strategy and the wet drying air and hot dry grains internal energy recovery strategy when drying air and condensed liquid water leave the heat exchangers. Methane consumption increases almost 21% when employing the wet drying air internal energy recovery strategy allowing only cooled drying air to leave the heat exchangers.

6. REFERENCES

Barrozo, M. A. S., H. M. Henrique, D. J. M. Sartori, and J. T. Freire, 2006, "The use of the orthogonal collocation method on the study of the drying kinetics of soybean seeds", Journal of Stored Products Research, 42, pp. 348–356.

Bejan, A., 1997, *Advanced engineering thermodynamics*, 2nd ed, John Wiley & Sons, Inc., New York, NY.

Lira, T. S., M. A. S. Barrozo, and A. J. Assis, 2009, "Concurrent moving bed dryer modeling: Sensitivity of physicochemical parameters and influence of air velocity profiles", Applied Thermal Engineering, 29, pp. 892 – 897.

Stanescu, G. and M. R. Errera, 2010, Grain drying finite time process optimization, Proceedings of the 7th International Conference on Heat Transfer, Fluid Mechanics and Thermodynamics, Antalya, Turkey, July 19-21.

7. RESPONSIBILITY NOTICE

The authors are the only responsible for the printed material included in this paper.